

Adaptive joint distribution learning

Damir Filipović* Michael Multerer† Paul Schneider‡

October 12, 2021

Abstract

We develop a new framework for embedding (joint) probability distributions in tensor product reproducing kernel Hilbert spaces (RKHS). This framework accommodates a low-dimensional, positive, and normalized model of a Radon-Nikodym derivative, estimated from sample sizes of up to several million data points, alleviating the inherent limitations of RKHS modeling. Well-defined normalized and positive conditional distributions are natural by-products to our approach. The embedding is fast to compute and naturally accommodates learning problems ranging from prediction to classification. The theoretical findings are supplemented by favorable numerical results.

1 Introduction

Embedding of (conditional) distributions in reproducing kernel Hilbert spaces (RKHS) has a long-standing tradition (Berlinet and Thomas-Agnan, 2004). It has been shown to be a highly effective machine learning technique in finite samples, with improved properties over local approaches used in extant nonparametric regressions (Grünwälder et al., 2012). Traditional embedding of distributions in RKHS is elegant and easily applied, and can be motivated from many different directions. For instance, Grünwälder et al. (2012) make a connection to the seminal vector-regression framework of Micchelli and Pontil (2005), Park and Muandet (2020) construct it from a measure-theoretic point of view, while Song et al. (2009) and Klebanov et al. (2020) derive it from operator theory.

However, the above-mentioned approaches suffer from several conceptual problems. They involve assumptions that are difficult to test. Estimates of probabilities are not guaranteed to be non-negative, and they are not normalized, rendering the RKHS distribution embedding problematic in many different situations of empirical

*EPFL AND SFI, damir.filipovic@epfl.ch

†UNIVERSITÀ DELLA SVIZZERA ITALIANA, michael.multerer@usi.ch

‡UNIVERSITÀ DELLA SVIZZERA ITALIANA AND SFI, paul.schneider@usi.ch

work. A conditional covariance matrix estimated with traditional RKHS distribution embedding, for instance, is not guaranteed to be positive semidefinite, and for higher dimensions in particular is unlikely to be.

In this paper we propose a new framework of RKHS embedding of distributions, similarly to [Schuster et al. \(2020a\)](#), with minimal assumptions, that comes with several advantages over the traditional construction. First, it has the oracle property in that it minimizes the distance to the true, unknown joint distribution, from which we are able to construct conditionals. It is engineered from a very generic tensor product RKHS setup and distinguishes between a potentially rough, but square-integrable prior distribution, and a (smoother) RKHS part. This enables us to represent, in particular, constants and independent distributions, that are both problematic for traditional distribution embeddings. Second, owing to the properties of the tensor product RKHS formulation, the embedding is normalized and non-negative in all states of the world, and thus satisfies the two defining structural properties of probability measures. This feature contrasts our approach to the traditional distribution embedding as mere projections of distributions that do not preserve these properties. To the best of our knowledge, only [Muzellec et al. \(2021\)](#) have considered these shape restrictions within embedding of distributions in RKHS. Third, we construct our distribution embedding directly in terms of an adaptive low-rank approximation by the pivoted Cholesky decomposition from [Bach and Jordan \(2002\)](#); [Beebe and Lindenberg \(1977\)](#); [Foster et al. \(2009\)](#); [Harbrecht et al. \(2012\)](#), with a sharply controlled a-posteriori error. This alleviates the curse of dimensionality, that usually necessitates an ad-hoc dimension reduction in RKHS modeling, and allows us to work with very large data sets.

The suggested embedding of distributions also naturally accommodates many problems not immediately associated with a probabilistic setting. For data $(x_1, y_1), \dots, (x_n, y_n)$, empirical objectives in machine learning with kernel methods in an RKHS \mathcal{H} are typically of the form

$$\frac{1}{n} \sum_{i=1}^n l(y_i; f(x_i)) + \lambda \|f\|_{\mathcal{H}}^2, \quad f \in \mathcal{H}, \lambda \geq 0, \quad (1)$$

for some loss function l . This specification is a regularized sample estimate of $\mathbb{E}[l(Y; \mathbb{E}[Y|X])]$ that can be directly evaluated with a model for the joint distribution of X and Y , like the one developed in this paper. Different operations on the same data, such as classification and interpolation, can thus be performed entirely consistently.

Section 2 introduces notation, and establishes positivity and normalization as the requirements defining probability distributions. In Section 3, we introduce our hypothesis space, our loss function and develop approximation results for finite-dimensional subspaces. Section 4 reviews tensor RKHS, and their computational properties, and develops results that enable us to ensure positivity and normalization within the subspace under consideration. Section 5 is devoted to numerical approx-

imation, in particular the adaptive low-rank representation by means of the pivoted Cholesky decomposition is discussed. Section 6 details our implementation. Section 7 shows extensive numerical experiments, and Section 8 concludes.

2 Preliminaries

Let X, Y be random variables taking values in some separable measurable spaces \mathcal{X} and \mathcal{Y} , respectively, with joint distribution \mathbb{P}_0 . Without loss of generality, we shall assume that $X(x, y) = x$ and $Y(x, y) = y$ are the canonical random variables defined on the product space $\mathcal{Z} := \mathcal{X} \times \mathcal{Y}$. The marginal distributions of X and Y on \mathcal{X} and \mathcal{Y} , are denoted by

$$\mathbb{P}_X(dx) = \mathbb{P}_0(dx, \mathcal{Y}) \quad \text{and} \quad \mathbb{P}_Y(dy) = \mathbb{P}_0(\mathcal{X}, dy), \quad (2)$$

respectively. We refer to the corresponding product measure on \mathcal{Z} by $\mathbb{P}_X \otimes \mathbb{P}_Y$. Moreover, for the sake of lighter notation, we introduce the abbreviations

$$L_{\mathbb{P}_0}^2 := L_{\mathbb{P}_0}^2(\mathcal{Z}; \mathbb{R}), \quad L_{\mathbb{P}_X}^2 := L_{\mathbb{P}_X}^2(\mathcal{X}; \mathbb{R}), \quad L_{\mathbb{P}_Y}^2 := L_{\mathbb{P}_Y}^2(\mathcal{Y}; \mathbb{R}),$$

and

$$L_{\mathbb{P}_X \otimes \mathbb{P}_Y}^2 := L_{\mathbb{P}_X \otimes \mathbb{P}_Y}^2(\mathcal{Z}; \mathbb{R})$$

and recall the isometric isomorphisms

$$L_{\mathbb{P}_X \otimes \mathbb{P}_Y}^2 = L_{\mathbb{P}_X}^2 \otimes L_{\mathbb{P}_Y}^2 = L_{\mathbb{P}_X}^2(\mathcal{X}; L_{\mathbb{P}_Y}^2) = L_{\mathbb{P}_Y}^2(\mathcal{Y}; L_{\mathbb{P}_X}^2). \quad (3)$$

Henceforth, we make the structural assumption that \mathbb{P}_0 is absolutely continuous with respect to the product measure $\mathbb{P}_X \otimes \mathbb{P}_Y$,

$$\mathbb{P}_0 \ll \mathbb{P}_X \otimes \mathbb{P}_Y. \quad (4)$$

We rely on the following elementary result.

Lemma 2.1. *The Radon-Nikodym derivative*

$$g_0 := \frac{d\mathbb{P}_0}{d(\mathbb{P}_X \otimes \mathbb{P}_Y)}$$

satisfies

$$\int_{\mathcal{Y}} g_0(\cdot, y) \mathbb{P}_Y(dy) = 1, \quad \mathbb{P}_X\text{-a.s.} \quad (5)$$

$$\int_{\mathcal{X}} g_0(x, \cdot) \mathbb{P}_X(dx) = 1, \quad \mathbb{P}_Y\text{-a.s.} \quad (6)$$

$$g_0 \geq 0, \quad \mathbb{P}_X \otimes \mathbb{P}_Y\text{-a.s.} \quad (7)$$

Conversely, given \mathbb{P}_X and \mathbb{P}_Y , every measurable function $g: \mathcal{Z} \rightarrow \mathbb{R}$ that satisfies (5)–(7) defines a probability measure \mathbb{P} on \mathcal{Z} satisfying (2) and (4) by setting

$$g = \frac{d\mathbb{P}}{d(\mathbb{P}_X \otimes \mathbb{P}_Y)}.$$

In this case, the conditional distributions of Y given $X = x$, and of X given $Y = y$, are given by

$$\mathbb{P}_{Y|X}(x, dy) = g(x, y)\mathbb{P}_Y(dy) \quad \text{and} \quad \mathbb{P}_{X|Y}(y, dx) = g(x, y)\mathbb{P}_X(dx). \quad (8)$$

Since it always holds that $\mathbb{P}(dx, dy) = \mathbb{P}_{Y|X}(x, dy)\mathbb{P}_X(dx)$ for a transition kernel $\mathbb{P}_{Y|X}(x, dy)$ from \mathcal{X} to \mathcal{Y} , the absolute continuity (4) is equivalent to assuming that

$$\mathbb{P}_{Y|X}(\cdot, dy) \ll \mathbb{P}_Y(dy), \quad \mathbb{P}_X\text{-a.s.}$$

Remark 2.2. *Introducing the linear embeddings*

$$\begin{aligned} I_X: L^2_{\mathbb{P}_X \otimes \mathbb{P}_Y} &\rightarrow L^2_{\mathbb{P}_X}, & I_X g &:= \int_{\mathcal{Y}} g(\cdot, y)\mathbb{P}_Y(dy) \\ I_Y: L^2_{\mathbb{P}_X \otimes \mathbb{P}_Y} &\rightarrow L^2_{\mathbb{P}_Y}, & I_Y g &:= \int_{\mathcal{X}} g(x, \cdot)\mathbb{P}_X(dx), \end{aligned} \quad (9)$$

we can rewrite the conditions (5) and (6) as

$$I_X g = 1 \quad \mathbb{P}_X\text{-a.s.} \quad \text{and} \quad I_Y g = 1 \quad \mathbb{P}_Y\text{-a.s.},$$

respectively.

3 Low-rank estimation of distributions

The overarching goal of this article is to learn the true population distribution \mathbb{P}_0 , and thus the conditional distributions (8) in particular, from observing a sample of (X, Y) , with the aid of low-rank kernel methods. A suitable hypothesis space that accommodates and facilitates this goal is given by the subsequent definition.

Definition 3.1. *Let E be a set and $(\mathcal{H}, \langle \cdot, \cdot \rangle_{\mathcal{H}})$ a Hilbert space of real-valued functions on E . Moreover, let $k: E \times E \rightarrow \mathbb{R}$ be a symmetric and positive semidefinite kernel, i.e., $[k(x_i, x_j)]_{i,j=1}^N$ is a symmetric and positive semidefinite matrix for each $N \in \mathbb{N}$ and $x_1, \dots, x_N \in E$. We call k a reproducing kernel for \mathcal{H} , iff $k(x, \cdot) \in \mathcal{H}$ for every $x \in E$ and $h(x) = \langle k(x, \cdot), h \rangle_{\mathcal{H}}$ for each $h \in \mathcal{H}$. In this case, we refer to \mathcal{H} as reproducing kernel Hilbert space (RKHS).*

In what follows, we shall assume that $(\mathcal{H}, \langle \cdot, \cdot \rangle_{\mathcal{H}})$ is a separable RKHS on \mathcal{Z} with measurable and bounded reproducing kernel k . As a consequence, the canonical embeddings

$$J_0: \mathcal{H} \rightarrow L^2_{\mathbb{P}_0}, \quad \text{and} \quad J: \mathcal{H} \rightarrow L^2_{\mathbb{P}_X \otimes \mathbb{P}_Y},$$

are Hilbert-Schmidt operators with adjoints

$$\begin{aligned} J_0^* f &= \int_{\mathcal{Z}} k(\cdot, z) f(z) \mathbb{P}_0(dz), \quad f \in L^2_{\mathbb{P}_0}, \\ J^* g &= \int_{\mathcal{Z}} k(\cdot, z) g(z) (\mathbb{P}_X \otimes \mathbb{P}_Y)(dz), \quad g \in L^2_{\mathbb{P}_X \otimes \mathbb{P}_Y}. \end{aligned}$$

In particular, the product

$$JJ^*: L^2(\mathcal{Z}, \mathbb{P}_X \otimes \mathbb{P}_Y) \rightarrow L^2(\mathcal{Z}, \mathbb{P}_X \otimes \mathbb{P}_Y), \quad JJ^* v = \int_{\mathcal{Z}} k(\cdot, z) v(z) (\mathbb{P}_X \otimes \mathbb{P}_Y)(dz),$$

is symmetric and of trace class with non-negative eigenvalues (see [Schatten, 1960](#)). We denote its trace by

$$\text{Tr}(JJ^*) := \sum_{i=1}^{\infty} (JJ^* \psi_i, \psi_i)_{L^2_{\mathbb{P}_X \otimes \mathbb{P}_Y}} = \sum_{i=1}^{\infty} \lambda_i = \int_{\mathcal{Z}} k(z, z) (\mathbb{P}_X \otimes \mathbb{P}_Y)(dz), \quad (10)$$

where $\{\psi_i\} \subset L^2_{\mathbb{P}_X \otimes \mathbb{P}_Y}$ is any orthonormal basis and $\lambda_1 \geq \lambda_2 \geq \dots \geq 0$ are the eigenvalues of JJ^* . Furthermore, we remark that the reproducing kernel exhibits an orthogonal expansion given by

$$k(z, z') = \sum_{i=1}^{\infty} \lambda_i \psi_i(z) \psi_i(z'), \quad (11)$$

where ψ_i are now the eigenfunctions of JJ^* .

The next straightforward result lies at the heart of our approach.

Lemma 3.2. *We have $J_0^* f = J^*(f g_0)$ for all $f \in L^2_{\mathbb{P}_0}$.*

Typically, RKHS do not contain the constant function (for instance [Minh, 2010](#), shows that for the widely used Gaussian RKHS). Thus, since the object of our interest is a Radon-Nikodym derivative, which takes the value one on average, we introduce the additive splitting

$$g = p + Jh, \quad (12)$$

where we think of p as a prior distribution that satisfies $I_X p = I_Y p = 1$. This implies that, if constant, p has to take the value one.

It remains to introduce a suitable measure of distance between \mathbb{P}_0 and $(p + Jh)(\mathbb{P}_X \otimes \mathbb{P}_Y)$ that can be empirically evaluated. To this end we consider the distance of the Radon-Nikodym derivatives g_0 and g for each function $f \in L^2_{\mathbb{P}_X \otimes \mathbb{P}_Y}$,

$$\begin{aligned} & \sup_{\|f\|_{L^2_{\mathbb{P}_X \otimes \mathbb{P}_Y}} \leq 1} \left| \int_{\mathcal{Z}} f \mathbb{P}_0(dz) - \int_{\mathcal{Z}} f(p + Jh)(\mathbb{P}_X \otimes \mathbb{P}_Y)(dz) \right| \\ &= \sup_{\|f\|_{L^2_{\mathbb{P}_X \otimes \mathbb{P}_Y}} \leq 1} |\langle f, g_0 - p - Jh \rangle_{L^2_{\mathbb{P}_X \otimes \mathbb{P}_Y}}| = \|g_0 - p - Jh\|_{L^2_{\mathbb{P}_X \otimes \mathbb{P}_Y}}. \end{aligned} \quad (13)$$

The expression above measures the worst-case loss. Moreover, if g is essentially bounded and the Radon-Nikodym derivative of \mathbb{P}_0 with respect to \mathbb{P} exists, it is an upper bound for the χ^2 divergence, and hence also for the Kullback-Leibler divergence. From the left-hand side of (13), it also has the oracle property in the sense that it depends on the unobservable population Radon-Nikodym derivative g_0 . For computational purposes, this can be mitigated by the decomposition

$$\|g_0 - p - Jh\|_{L^2_{\mathbb{P}_X \otimes \mathbb{P}_Y}}^2 = \|g_0 - p\|_{L^2_{\mathbb{P}_X \otimes \mathbb{P}_Y}}^2 - 2\langle J_0^*1 - J^*p, h \rangle_{\mathcal{H}} + \langle J^*Jh, h \rangle_{\mathcal{H}},$$

that can be derived from Lemma 3.2. Adding ridge-type regularization, we finally arrive at the objective

$$\|g_0 - p - Jh\|_{L^2_{\mathbb{P}_X \otimes \mathbb{P}_Y}}^2 + \lambda \|h\|_{\mathcal{H}}^2. \quad (14)$$

Minimizing (14) can therefore be reduced to minimizing

$$-2\langle J_0^*1 - J^*p, h \rangle_{\mathcal{H}} + \langle (J^*J + \lambda)h, h \rangle_{\mathcal{H}}.$$

Kernel methods are notoriously susceptible to large sample sizes. With big data in mind, we therefore directly solve problem (14) on a suitable m -dimensional subspace $V \subseteq \mathcal{H}$ with $V = \text{span}\{\phi_1, \dots, \phi_m\}$, where we introduce the row vector $\phi_m := [\phi_1, \dots, \phi_m]$ for notational convenience. This way, we may write a function $h \in V$ simply as

$$h = \sum_{i=1}^m h_i \phi_i = \phi_m \mathbf{h}$$

with the coefficient vector $\mathbf{h} := [h_1, \dots, h_m]^\top \in \mathbb{R}^m$. Our particular choice of this subspace will be discussed later on in Section 5.

Remark 3.3. *Deriving a representer theorem for the infinite-dimensional case $V = \mathcal{H}$ poses technical difficulties due to the positivity constraint. We remark, however, that for the finite dimensional case as it emerges under the sample distribution, a constraint representer theorem has already been derived in Koppel et al. (2019).*

With the decomposition of the objective (14) at hand, we arrive at

$$\underset{\mathbf{h} \in \mathbb{R}^m \text{ s.t. (5), (6), (7)}}{\text{minimize}} \quad -2\langle J_0^*1 - J^*p, \phi_m \rangle_{\mathcal{H}} \mathbf{h} + \mathbf{h}^\top \langle (J^*J + \lambda) \phi_m^\top, \phi_m \rangle_{\mathcal{H}} \mathbf{h}. \quad (15)$$

For the sake of completeness, we also consider an unconstrained version of (15) that minimizes the same objective, but without taking into account the constraints (5), (6), and (7), as well as a version that is only normalized through constraints (5) and (6), but does not impose positivity.

The quality of the solution to the finite-dimensional optimization problems (15) and its unconstrained counterpart, respectively, will typically depend on the approximation properties of the underlying space V , that induces the reproducing kernel

$$k_V(z, z') = \phi_m(z) \mathbf{G}^{-1} \phi_m^\top(z'),$$

with $\mathbf{G} := \langle \phi_m^\top, \phi_m \rangle_{\mathcal{H}} \in \mathbb{R}^{m \times m}$ being the Gram matrix associated to ϕ_m (see Berlinet and Thomas-Agnan, 2004). In particular, there holds

$$\langle k_V(z, \cdot), v \rangle_{\mathcal{H}} = v(z), \quad \text{for all } v \in V,$$

and we can introduce the canonical embedding $J_V: V \rightarrow L^2_{\mathbb{P}_X \otimes \mathbb{P}_Y}$ with adjoint

$$J_V^* g = J_V J_V^* g = \int_{\mathcal{Z}} k_V(\cdot, z) g(z) (\mathbb{P}_X \otimes \mathbb{P}_Y)(dz), \quad g \in L^2_{\mathbb{P}_X \otimes \mathbb{P}_Y}.$$

We obtain the following approximation result

Theorem 3.4. *Let $h \in \mathcal{H}$ and $h_V \in V$ be its \mathcal{H} -orthogonal projection onto V . Then, it holds*

$$\|h - h_V\|_{L^2_{\mathbb{P}_X \otimes \mathbb{P}_Y}} \leq \|h\|_{\mathcal{H}} \sqrt{\text{Tr}(JJ^* - J_V J_V^*)}.$$

Proof. The best approximation of $h \in \mathcal{H}$ in V is given by the \mathcal{H} -orthogonal projection. It is easy to see that the set $\psi_m = [\psi_1, \dots, \psi_m] := [\phi_1, \dots, \phi_m] \mathbf{G}^{-1/2}$ forms an orthonormal basis of V . Hence, the orthogonal projection of h can be written as

$$h_V = \psi_m \langle \psi_m^\top, h \rangle_{\mathcal{H}} = \phi_m \mathbf{G}^{-1} \langle \phi_m^\top, h \rangle_{\mathcal{H}},$$

i.e.,

$$h_V(z) = \langle k_V(z, \cdot), h \rangle_{\mathcal{H}}.$$

Furthermore, it holds for $z \in \mathcal{Z}$ that

$$\begin{aligned} (h(z) - h_V(z))^2 &= (\langle k(z, \cdot), h \rangle_{\mathcal{H}} - \langle k_V(z, \cdot), h \rangle_{\mathcal{H}})^2 = (\langle k(z, \cdot) - k_V(z, \cdot), h \rangle_{\mathcal{H}})^2 \\ &\leq \|k(z, \cdot) - k_V(z, \cdot)\|_{\mathcal{H}}^2 \|h\|_{\mathcal{H}}^2, \end{aligned}$$

where the last step follows from the Cauchy-Schwartz inequality. Next, we observe that

$$\|k(z, \cdot) - k_V(z, \cdot)\|_{\mathcal{H}}^2 = k(z, z) - k_V(z, z).$$

Hence, to complete the proof, we need to show that $k(z, z) - k_V(z, z)$ is a positive semidefinite kernel. To this end, we extend the orthonormal basis $\boldsymbol{\psi}_m$ of V to an orthonormal basis $\boldsymbol{\psi}$ of \mathcal{H} . Then, Parseval's identity yields for any $z_i, z_j \in \mathcal{Z}$ that

$$\begin{aligned}
k(z_i, z_j) - k_V(z_i, z_j) &= k(z_i, z_j) - \boldsymbol{\psi}_m(z_i) \boldsymbol{\psi}_m^\top(z_j) \\
&= \langle k(z_i, \cdot), k(z_j, \cdot) \rangle_{\mathcal{H}} - \sum_{t=1}^m \langle k(z_i, \cdot), \psi_t \rangle_{\mathcal{H}} \langle k(z_j, \cdot), \psi_t \rangle_{\mathcal{H}} \\
&= \sum_{t=1}^{\infty} \langle k(z_i, \cdot), \psi_t \rangle_{\mathcal{H}} \langle k(z_j, \cdot), \psi_t \rangle_{\mathcal{H}} - \sum_{t=1}^m \langle k(z_i, \cdot), \psi_t \rangle_{\mathcal{H}} \langle k(z_j, \cdot), \psi_t \rangle_{\mathcal{H}} \\
&= \sum_{t=m+1}^{\infty} \psi_t(z_i) \psi_t(z_j).
\end{aligned}$$

Thus, it holds for any $n \in \mathbb{N}$, $c_1, \dots, c_n \in \mathbb{R}$ and $z_1, \dots, z_n \in \mathcal{Z}$ that

$$\begin{aligned}
\sum_{i,j=1}^n c_i c_j (k(z_i, z_j) - k_V(z_i, z_j)) &= \sum_{i,j=1}^n c_i c_j \sum_{t=m+1}^{\infty} \psi_t(z_i) \psi_t(z_j) \\
&= \sum_{t=m+1}^{\infty} \left(\sum_{i=1}^n c_i \psi_t(z_i) \right)^2 \geq 0,
\end{aligned}$$

which establishes the positive definiteness. Therefore, we finally arrive at

$$\begin{aligned}
\|h - h_V\|_{L_{\mathbb{P}_X \otimes \mathbb{P}_Y}^2}^2 &\leq \|h\|_{\mathcal{H}}^2 \int_{\mathcal{Z}} (k(z, z) - k_V(z, z)) (\mathbb{P}_X \otimes \mathbb{P}_Y)(dz) \\
&= \|h\|_{\mathcal{H}}^2 \text{Tr}(JJ^* - J_V J_V^*).
\end{aligned}$$

□

With regard to (10), the theorem immediately suggests that the approximation space is chosen as the dominant subspace of JJ^* . We have the following corollary.

Corollary 3.5. *The error $\|h - h_V\|_{L_{\mathbb{P}_X \otimes \mathbb{P}_Y}^2}$ is minimized by choosing V as the m -dimensional dominant subspace of JJ^* . In this case,*

$$\|h - h_V\|_{L_{\mathbb{P}_X \otimes \mathbb{P}_Y}^2} \leq \|h\|_{\mathcal{H}} \sqrt{\sum_{i=m+1}^{\infty} \lambda_i}.$$

Proof. For the L^2 -orthonormal eigenfunctions $\{\psi_i\}$ of JJ^* there holds

$$\langle \psi_{i'}, \psi_i \rangle_{\mathcal{H}} = \begin{cases} \lambda_i^{-1}, & i = i', \\ 0, & \text{else,} \end{cases}$$

see, for example, [Boudabsa and Filipović \(2019\)](#). Thus, in view of (11), setting

$$k_V(z, z') = \boldsymbol{\psi}_m(z) \mathbf{G}^{-1} \boldsymbol{\psi}_m^\top(z') = \sum_{i=1}^m \lambda_i \psi_i(z) \psi_i(z'), \quad \text{where } \mathbf{G} = \langle \boldsymbol{\psi}_m^\top, \boldsymbol{\psi}_m \rangle_{\mathcal{H}},$$

yields the assertion. \square

Another important consequence of the theorem is that the approximation is monotonic in the sense that extending the subspace does not worsen the error bound.

Corollary 3.6. *Let $V \subset \tilde{V} \subset \mathcal{H}$ be two subspaces and denote for $h \in \mathcal{H}$ by $h_{\tilde{V}} \in \tilde{V}$ its \mathcal{H} -orthogonal projection onto \tilde{V} . Then, there holds*

$$\|h - h_{\tilde{V}}\|_{L^2_{\mathbb{P}_X \otimes \mathbb{P}_Y}} \leq \|h\|_{\mathcal{H}} \sqrt{\text{Tr}(JJ^* - J_V J_V^*)}.$$

Proof. With similar arguments as used in the proof of Theorem 3.4, it can be inferred that $k_{\tilde{V}} = k_V + k_W$, where $W \subset \tilde{V}$ is the \mathcal{H} -orthogonal complement of V in \tilde{V} . In particular, k_W is a positive semidefinite kernel. Hence, we have

$$\text{Tr}(J_V J_V^*) \leq \text{Tr}(J_V J_V^*) + \text{Tr}(J_W J_W^*) = \text{Tr}(J_{\tilde{V}} J_{\tilde{V}}^*).$$

Therefore, it holds

$$\|h - h_{\tilde{V}}\|_{L^2_{\mathbb{P}_X \otimes \mathbb{P}_Y}}^2 \leq \|h\|_{\mathcal{H}}^2 \text{Tr}(JJ^* - J_{\tilde{V}} J_{\tilde{V}}^*) \leq \|h\|_{\mathcal{H}}^2 \text{Tr}(JJ^* - J_V J_V^*).$$

The claim is now obtained by taking square roots. \square

4 Tensor product kernels

The approximation problem considered in this article amounts to the approximation of the Radon-Nikodym derivative $g(x, y)$ with $(x, y) \in \mathcal{X} \times \mathcal{Y}$. Hence, a natural candidate is a RKHS which is of tensor product structure, as described for instance in [Berlinet and Thomas-Agnan \(2004\)](#). Concretely, we consider the tensor product kernel $k = k_X \otimes k_Y$, that is,

$$k((x, y), (x', y')) := k_X(x, x') k_Y(y, y') \quad x, x' \in \mathcal{X}, \quad y, y' \in \mathcal{Y}, \quad (16)$$

where k_X and k_Y are kernels defined on \mathcal{X} and \mathcal{Y} , respectively. The corresponding RKHS \mathcal{H} is isometrically isomorphic to the tensor product $\mathcal{H}_X \otimes \mathcal{H}_Y$ of the RKHS \mathcal{H}_X and \mathcal{H}_Y , see, e.g., [Paulsen and Raghupathi \(2016\)](#) for details.

As $\mathcal{H}_X, \mathcal{H}_Y$ are both separable, they are spanned by countable orthonormal bases $\boldsymbol{\psi}_X := [\psi_{X,1}, \psi_{X,2}, \dots]$ and $\boldsymbol{\psi}_Y := [\psi_{Y,1}, \psi_{Y,2}, \dots]$. In particular, we represent every $h \in \mathcal{H}_X \otimes \mathcal{H}_Y$ according to

$$h = \sum_{i=1}^{\infty} \sum_{j=1}^{\infty} h_{j,i} \psi_{X,i} \otimes \psi_{Y,j} = \boldsymbol{\psi}_Y \mathbf{H} \boldsymbol{\psi}_X^\top$$

with the bi-infinite matrix $\mathbf{H} := [h_{j,i}]_{i,j=1}^\infty \in \ell^2(\mathbb{N}^2)$. We obtain the Hilbert-Schmidt embeddings

$$J_X: \mathcal{H}_X \rightarrow L_{\mathbb{P}_X}^2 \quad \text{and} \quad J_Y: \mathcal{H}_Y \rightarrow L_{\mathbb{P}_Y}^2$$

with adjoints

$$J_X^* f(x) = \int_{\mathcal{X}} k_X(x, x') f(x') \mathbb{P}_X(dx') \quad \text{and} \quad J_Y^* f(y) = \int_{\mathcal{Y}} k_Y(y, y') f(y') \mathbb{P}_Y(dy'),$$

for $f \in L_{\mathbb{P}_X}^2$ and $f \in L_{\mathbb{P}_Y}^2$, respectively. Combining this with (3) and (8), any g that satisfies (5) through (7) yields kernel embeddings of the corresponding conditional distributions $\mathbb{P}_{Y|X}(x, dy)$ and $\mathbb{P}_{X|Y}(y, dx)$, in the sense that

$$\begin{aligned} \int_{\mathcal{Y}} f(y) \mathbb{P}_{Y|X}(x, dy) &= \langle f, J_Y^* g(x, \cdot) \rangle_{\mathcal{H}_Y} \quad \text{and} \\ \int_{\mathcal{X}} f(x) \mathbb{P}_{X|Y}(y, dx) &= \langle f, J_X^* g(\cdot, y) \rangle_{\mathcal{H}_X}, \end{aligned} \tag{17}$$

for $f \in \mathcal{H}_Y$ and $f \in \mathcal{H}_X$, respectively.

As we see from (17), the conditional distributions $\mathbb{P}_{Y|X}(x, dy)$ and $\mathbb{P}_{X|Y}(y, dx)$ are not simply given by linear operations on the kernels k_Y and k_X . This seems to be in contradiction to the large literature on kernel embeddings of conditional distributions, such as Schuster et al. (2020b). However, we conjecture that the assumptions about the kernel embedding of the Dirac measures being in the domain of the conditional mean operator $\mathcal{U}_{Y|X}$ in Schuster et al. (2020b) are very restrictive and not satisfied in general. In turn, the numerical representation of the resulting conditional density operator produces signed measures, that are not normalized. We further remark that this linear theory corresponds, at best, to our unconstrained problem. Only if the minimizer of (15) satisfies (5), (6), (7) we do obtain a bona fide conditional distribution.

For the remainder of this section, we elaborate on the normalization and the positivity of the estimated density, that emerge naturally in the tensor product kernel case. To this end, we assume that the approximation space is given by

$$V = V_X \otimes V_Y$$

with $\dim(V_X) = m_X$ and $\dim(V_Y) = m_Y$, i.e., $m = m_X \cdot m_Y$. In particular, given orthonormal bases ψ_X of V_X and ψ_Y of V_Y , respectively, an orthonormal basis for V is given by $\psi_m = \psi_X \otimes \psi_Y$, where in the case of matrices the tensor product is given by the Kronecker product. The latter is defined for two matrices $\mathbf{A} \in \mathbb{R}^{m \times n}$ and $\mathbf{A}' \in \mathbb{R}^{m' \times n'}$ according to

$$\mathbf{A} \otimes \mathbf{A}' := \begin{bmatrix} a_{1,1} \mathbf{A}' & \cdots & a_{1,n} \mathbf{A}' \\ \vdots & \ddots & \vdots \\ a_{m,1} \mathbf{A}' & \cdots & a_{m,n} \mathbf{A}' \end{bmatrix} \in \mathbb{R}^{(mm') \times (nn')}.$$

Consequently, every function $h_V \in V$ can be written as

$$h_V = \sum_{i=1}^{m_X} \sum_{j=1}^{m_Y} h_{j,i} (\psi_{X,i} \otimes \psi_{Y,j}) = \boldsymbol{\psi}_Y \mathbf{H} \boldsymbol{\psi}_X^\top = (\boldsymbol{\psi}_X \otimes \boldsymbol{\psi}_Y) \text{vec}(\mathbf{H}) = \boldsymbol{\psi}_m \mathbf{h}, \quad (18)$$

with coefficient matrix $\mathbf{H} \in \mathbb{R}^{m_Y \times m_X}$. Herein, $\mathbf{h} = \text{vec}(\mathbf{H}) \in \mathbb{R}^{m_Y \cdot m_X}$ is the vector which is obtained by concatenating the columns of \mathbf{H} .

With these definitions at hand, we start by stating a, perhaps surprising, result that delivers a finite-dimensional condition for the infinite-dimensional constraints (5) and (6).

Lemma 4.1 (Normalization). *Let $I_X p = I_Y p = 1$, cp. (9), and $k = k_X \otimes k_Y$. Then, conditions (5) and (6) are satisfied for $g = p + h$ with $h = \boldsymbol{\psi}_Y \mathbf{H} \boldsymbol{\psi}_X^\top \in V$, for $\mathbf{H} \in \mathbb{R}^{m_Y \times m_X}$, if*

$$(I_X \boldsymbol{\psi}_Y) \mathbf{H} = \mathbf{0} \quad \text{and} \quad \mathbf{H} (I_Y \boldsymbol{\psi}_X)^\top = \mathbf{0}. \quad (19)$$

If, moreover, $\boldsymbol{\psi}_X$ and $\boldsymbol{\psi}_Y$ are linearly independent in $L_{\mathbb{P}_X}^2$ and $L_{\mathbb{P}_Y}^2$, respectively, then (19) is also necessary for (5) and (6).

Proof. We give here the argument for X -conditional expectations. The Y -conditional expectations can be derived analogously. It holds

$$I_X g = I_X p + I_X h = 1 + (I_X \boldsymbol{\psi}_Y) \mathbf{H} \boldsymbol{\psi}_X^\top,$$

so that condition (5) reads as

$$(I_X \boldsymbol{\psi}_Y) \mathbf{H} \boldsymbol{\psi}_X^\top = 0 \quad \mathbb{P}_X\text{-a.s.}$$

□

Next we elaborate on the positivity constraint (7). As the reproducing kernels under consideration are bounded, it is a natural assumption that this carries over also to the basis $\{\phi_1, \dots, \phi_m\} \subset V$. For example, the Newton basis discussed in Müller and Schaback (2009) has this property. Without loss of generality, we assume that $\phi_i(z) \in [a_i, b_i]$, $z \in \mathcal{Z}$, $a_i < b_i$ for all $i = 1, \dots, m$, and we set $C := \times_{i=1}^m [a_i, b_i]$. We refer to the subsequent Section 5 for concrete bounds of the bases under consideration. We further remark that positivity through sum of squares condition imposed through semidefinite programming as in Marteau-Ferey et al. (2020) and Muzellec et al. (2021), and unbounded polynomial kernels as in Almeida and Schneider (2021), do not scale well with the number of data points.

In our setting with bounded kernels, we are interested in the set

$$\mathcal{P} := \{\mathbf{h} \in \mathbb{R}^m \mid \min_{\mathbf{x} \in C} \mathbf{x}^\top \mathbf{h} + p \geq 0\}$$

to ensure positivity. Decomposing $\text{vec}(\mathbf{H}) = \mathbf{h}^+ - \mathbf{h}^-$, with $\mathbf{h}_i^-, \mathbf{h}_i^+ \geq 0$, we can state the following

Lemma 4.2 (Positivity for bounded kernels). *It holds $\text{vec}(\mathbf{H}) \in \mathcal{P}$ if and only if*

$$\mathbf{a}^\top \mathbf{h}^+ - \mathbf{b}^\top \mathbf{h}^- + p \geq 0. \quad (20)$$

In this case, (7) is satisfied for $g = p + h$ with h given in (18).

Proof. As it is always true that $a_i h_i^+ - b_i h_i^- \leq h_i x_i$ for all $x_i \in [a_i, b_i]$, in particular also for the minimum, $\text{vec}(\mathbf{H})$ satisfying condition (20) is equivalent to its membership to \mathcal{P} . \square

In sum, we obtain sufficient conditions (19) and (20) for the normality constraints (5) and (6) and the positivity constraint (7), that are computationally more efficient when solving the constrained optimization problem (15), as we shall see in the following section.

5 Numerical approximation

For the numerical approximation of the sought density, we have to address the discretization of the probability measure on $L^2_{\mathbb{P}_X \otimes \mathbb{P}_Y}$ on the one hand, and to provide a means to determine a suitable subspace $V \subset \mathcal{H}$ on the other hand. For a given training sample $(x_1, y_1), \dots, (x_n, y_n) \subset \mathcal{Z}$ drawn from \mathbb{P}_0 , we define the empirical distribution

$$\widehat{\mathbb{P}}_0 := \frac{1}{n} \sum_{i=1}^n \delta_{(x_i, y_i)},$$

and the marginal distributions

$$\widehat{\mathbb{P}}_X := \frac{1}{n} \sum_{i=1}^n \delta_{x_i} \quad \text{and} \quad \widehat{\mathbb{P}}_Y := \frac{1}{n} \sum_{i=1}^n \delta_{y_i}.$$

In particular, there holds

$$\widehat{\mathbb{P}_X \otimes \mathbb{P}_Y} = \widehat{\mathbb{P}}_X \otimes \widehat{\mathbb{P}}_Y = \frac{1}{n^2} \sum_{i,j=1}^n \delta_{(x_i, y_j)}.$$

We further denote the corresponding estimated Hilbert-Schmidt embeddings by

$$\widehat{J}_0: \mathcal{H} \rightarrow L^2_{\widehat{\mathbb{P}}_0} \quad \text{and} \quad \widehat{J}: \mathcal{H} \rightarrow L^2_{\widehat{\mathbb{P}_X \otimes \mathbb{P}_Y}},$$

and identify a function $f \in L^2_{\widehat{\mathbb{P}}_0}$ with the n -vector $\mathbf{f} = [f(x_i, y_i)]_{i=1}^n$, while $g \in L^2_{\widehat{\mathbb{P}_X \otimes \mathbb{P}_Y}}$ is represented by the $n \times n$ -matrix $\mathbf{g} = [g(x_i, y_j)]_{i,j=1}^n$.

The evaluations of the Hilbert-Schmidt embeddings under the empirical distributions $\widehat{\mathbb{P}}_0$ and $\widehat{\mathbb{P}}_X \otimes \widehat{\mathbb{P}}_Y$ are then given according to

$$\widehat{J}_0^* 1(x, y) = \frac{1}{n} \sum_{i=1}^n k((x, y), (x_i, y_i)), \quad (21)$$

$$\widehat{J}^* g(x, y) = \frac{1}{n^2} \sum_{i,j=1}^n k((x, y), (x_i, y_j)) g_{i,j}, \quad (22)$$

$$(\widehat{J}_0 \widehat{J}_0^* 1)_i = \frac{1}{n} \sum_{j=1}^n k((x_i, y_i), (x_j, y_j)), \quad (23)$$

$$(\widehat{J} \widehat{J}_0^* 1)_{i,j} = \frac{1}{n} \sum_{s=1}^n k((x_i, y_j), (x_s, y_s)), \quad (24)$$

$$(\widehat{J} \widehat{J}^* g)_{i,j} = \frac{1}{n^2} \sum_{s,t=1}^n k((x_i, y_j), (x_s, y_t)) g_{s,t}. \quad (25)$$

Solving problem (14) for a finite sample does not scale well with respect to the sample size n . This is particularly true for our approach, since (25) suggests that the kernel matrix

$$\mathbf{K} = [k((x_i, y_j), (x_s, y_t))]_{i,j,s,t=1}^n \in \mathbb{R}^{N \times N},$$

which represents $\widehat{J} \widehat{J}^*$, is of size $N \times N$ with $N := n^2$. Especially, computing the spectral decomposition of \mathbf{K} in order to choose the approximation space V equal to the dominant subspace can easily become prohibitive, as the cost for solving the corresponding eigenvalue problem is $\mathcal{O}(N^3)$. Therefore, we rather require an approach that, given N sample points, extracts a suitable subsample $z_{i_1}, \dots, z_{i_m} \in \mathcal{Z}$. Given the subsample, we consider the space $V = \text{span}\{\phi_{i_1}, \dots, \phi_{i_m}\}$ with

$$\phi_j := k(z_j, \cdot), \quad j = 1, \dots, N.$$

In order to actually compute V , we resort to a greedy strategy which reduces the trace of the kernel matrix in an iterative fashion. Such a greedy strategy is provided by the diagonally pivoted Cholesky decomposition, which indeed coincides with total pivoting. The procedure is summarized using MATLAB notation in Algorithm 1.

By means of a slight modification of Algorithm 1, we can directly obtain the basis $\mathbf{b}_1, \dots, \mathbf{b}_m$ which is biorthogonal to ℓ_1, \dots, ℓ_m . This modified procedure can be found in Algorithm 2.

Theorem 5.1. *Algorithm 2 works correctly.*

Proof. To show the correctness, let p_m denote the column index of the pivot element in the m -th step of Algorithm 2. Moreover, for the sake of convenience, we define $\mathbf{B}_m := [\mathbf{b}_1, \dots, \mathbf{b}_m]$ and $\mathbf{L}_m := [\ell_1, \dots, \ell_m]$. It holds

$$\mathbf{b}_1 = \frac{1}{\ell_{1,p_1}} (\mathbf{e}_{p_1} - \mathbf{B}_0 \mathbf{L}_0^\top(:, p_1)) = \frac{1}{\ell_{1,p_1}} \mathbf{e}_{p_1} = \mathbf{K}^{-1} \ell_1.$$

Algorithm 1 pivoted Cholesky decomposition

input: symmetric and positive semidefinite matrix $\mathbf{K} \in \mathbb{R}^{N \times N}$,
tolerance $\varepsilon > 0$

output: low-rank approximation $\mathbf{K} \approx \mathbf{L}\mathbf{L}^\top$

- 1: Initialization: set $m := 1$, $\mathbf{d} := \text{diag}(\mathbf{K})$, $\text{err} := \|\mathbf{d}\|_1$
- 2: **while** $\text{err} > \varepsilon$
- 3: determine $j := \arg \max_{1 \leq i \leq N} d_i$
- 4: compute $\hat{\boldsymbol{\ell}}_m := \mathbf{K}(:, j) - \mathbf{L} * \mathbf{L}^\top(:, j)$
- 5: set $\boldsymbol{\ell}_m := \hat{\boldsymbol{\ell}}_m / \sqrt{d_j}$
- 6: set $\mathbf{L} := [\mathbf{L}, \boldsymbol{\ell}_m]$
- 7: set $\mathbf{d} := \mathbf{d} - \boldsymbol{\ell}_m * \boldsymbol{\ell}_m$
- 8: set $\text{err} := \|\mathbf{d}\|_1$
- 9: set $m := m + 1$

Now, let the assertion be satisfied for some $m - 1 \geq 1$. Then it holds

$$\begin{aligned}
\mathbf{b}_m &= \frac{1}{\ell_{m,p_m}} (\mathbf{e}_{p_m} - \mathbf{B}_{m-1} \mathbf{L}_{m-1}^\top(:, p_m)) = \frac{1}{\ell_{m,p_m}} (\mathbf{e}_{p_m} - \mathbf{L}_N^{-\top} [\mathbf{e}_1, \dots, \mathbf{e}_{m-1}] \mathbf{L}_{m-1}^\top(:, p_m)) \\
&= \frac{1}{\ell_{m,p_m}} (\mathbf{e}_{p_m} - \mathbf{L}_N^{-\top} \mathbf{L}_N^{-1} \mathbf{L}_{m-1} \mathbf{L}_{m-1}^\top(:, p_m)) = \frac{1}{\ell_{m,p_m}} \mathbf{K}^{-1} (\mathbf{K} \mathbf{e}_{p_m} - \mathbf{L}_{m-1} \mathbf{L}_{m-1}^\top(:, p_m)) \\
&= \mathbf{K}^{-1} \left(\frac{1}{\ell_{m,p_m}} (\mathbf{K}(:, p_m) - \mathbf{L}_{m-1} \mathbf{L}_{m-1}^\top(:, p_m)) \right) = \mathbf{K}^{-1} \boldsymbol{\ell}_m.
\end{aligned}$$

Note that we exploit here that the columns of \mathbf{B}_{m-1} exactly coincide with the first $m - 1$ rows of \mathbf{L}_N^{-1} .

By concatenating the vectors, this proves $\mathbf{B}_m = \mathbf{K}^{-1} \mathbf{L}_m$ for $m = 1, \dots, N$. In particular, it holds now

$$\mathbf{B}_m^\top \mathbf{L}_m = \mathbf{L}_m^\top \mathbf{K}^{-1} \mathbf{L}_m = \mathbf{L}_m^\top \mathbf{L}_N^{-\top} \mathbf{L}_N^{-1} \mathbf{L}_m = [\mathbf{e}_1^\top, \dots, \mathbf{e}_m^\top]^\top [\mathbf{e}_1, \dots, \mathbf{e}_m] = \mathbf{I}_m.$$

which proves the biorthogonality. \square

Matrix \mathbf{B} can be employed to transform the linearly independent functions $\phi_{i_1}, \dots, \phi_{i_m}$ into an orthonormal basis for $V = \text{span}\{\phi_{i_1}, \dots, \phi_{i_m}\}$. This basis is constructed via $\mathbf{N} := [\phi_1, \dots, \phi_N] \mathbf{B}$, and is known as Newton basis in literature, see Müller and Schaback (2009); Pazouki and Schaback (2011). In particular, in Pazouki and Schaback (2011) a construction similar to the one above is suggested.

Theorem 5.2. *Let $\boldsymbol{\phi} = [\phi_1, \dots, \phi_N]$ and $V_\varepsilon = \text{span}\{\phi_{i_1}, \dots, \phi_{i_m}\}$, where the indices i_1, \dots, i_m have been selected by Algorithm 2. Then, it holds for $\psi_i := \boldsymbol{\phi} \mathbf{b}_i$, $i = 1, \dots, m$ that $V_\varepsilon = \text{span}\{\psi_1, \dots, \psi_m\}$ and*

$$\langle \psi_i, \psi_{i'} \rangle_{\mathcal{H}} = \delta_{i,i'}.$$

Algorithm 2 biorthogonal Cholesky basis

input: symmetric and positive semidefinite matrix $\mathbf{K} \in \mathbb{R}^{N \times N}$,
tolerance $\varepsilon > 0$

output: low-rank approximation $\mathbf{K} \approx \mathbf{L}\mathbf{L}^\top$
and biorthogonal basis \mathbf{B} such that $\mathbf{B}^\top \mathbf{L} = \mathbf{I}$

- 1: Initialization: set $m := 1$, $\mathbf{d} := \text{diag}(\mathbf{K})$, $\mathbf{L} := []$, $\mathbf{B} := []$, $\text{err} := \|\mathbf{d}\|_1$
- 2: **while** $\text{err} > \varepsilon$
- 3: determine $j := \arg \max_{1 \leq i \leq N} d_i$
- 4: compute $\hat{\boldsymbol{\ell}}_m := \mathbf{K}(:, j) - \mathbf{L} * \mathbf{L}^\top(:, j)$
- 5: compute $\hat{\mathbf{b}}_m := \mathbf{e}_j - \mathbf{B} * \mathbf{L}^\top(:, j)$
- 6: set $\boldsymbol{\ell}_m := \hat{\boldsymbol{\ell}}_m / \sqrt{d_j}$
- 7: set $\mathbf{b}_m := \hat{\mathbf{b}}_m / \sqrt{d_j}$
- 8: set $\mathbf{L} := [\mathbf{L}, \boldsymbol{\ell}_m]$
- 9: set $\mathbf{B} := [\mathbf{B}, \mathbf{b}_m]$
- 10: set $\mathbf{d} := \mathbf{d} - \boldsymbol{\ell}_m * \boldsymbol{\ell}_m$
- 11: set $\text{err} := \|\mathbf{d}\|_1$
- 12: set $m := m + 1$

Proof. We start by proving the orthonormality of the functions $\{\psi_i\}$. It holds

$$\langle \psi_i, \psi_{i'} \rangle_{\mathcal{H}} = \langle \phi \mathbf{b}_i, \phi \mathbf{b}_{i'} \rangle_{\mathcal{H}} = \left\langle \sum_{j=1}^N k(z_j, \cdot) b_{i,j}, \sum_{j'=1}^N k(z'_{j'}, \cdot) b_{i',j'} \right\rangle_{\mathcal{H}} = \mathbf{b}_i^\top \mathbf{K} \mathbf{b}_{i'} = \mathbf{e}_i^\top \mathbf{e}_{i'} = \delta_{i,i'}.$$

Next, we observe that $\mathbf{b}_j \in \text{span}\{\mathbf{e}_{i_1}, \dots, \mathbf{e}_{i_j}\}$ for some indices $i_1, \dots, i_j \in \{1, \dots, N\}$, cp. Algorithm 2. Thus, it holds $\psi_j \in \text{span}\{\phi_{i_1}, \dots, \phi_{i_j}\}$ and we infer

$$\text{span}\{\psi_1, \dots, \psi_m\} \subset \text{span}\{\phi_{i_1}, \dots, \phi_{i_m}\} = V_\varepsilon.$$

Now, due to the orthonormality of $\{\psi_i\}$, it even holds $V_\varepsilon = \text{span}\{\psi_1, \dots, \psi_m\}$ by a dimensionality argument. \square

Next, we derive a basis that is orthogonal with respect to the $L^2_{\widehat{\mathbb{P}}_X \otimes \widehat{\mathbb{P}}_Y}$ -inner product and with respect to the \mathcal{H} -inner product at the same time. To this end, we observe that $\mathbf{L} = \mathbf{K}(:, \mathbf{p})\mathbf{U}$, where \mathbf{U} is the inverse of the upper triangular Cholesky factor of $\mathbf{K}(\mathbf{p}, \mathbf{p}) \in \mathbb{R}^{m \times m}$, i.e. $[\mathbf{K}(\mathbf{p}, \mathbf{p})]^{-1} = \mathbf{U}\mathbf{U}^\top$. In particular, there holds

$$\mathbf{U}(i, :) = \mathbf{B}(p_i, :), \quad i = 1, \dots, m,$$

i.e. the matrix \mathbf{U} contains the compressed columns of \mathbf{B} . Thus, choosing the basis

$$\psi_i := \phi_{\mathbf{p}} \mathbf{U} \mathbf{v}_i = \phi \mathbf{B} \mathbf{v}_i, \quad (26)$$

where $\mathbf{L}^\top \mathbf{L} = \mathbf{V} \mathbf{\Lambda} \mathbf{V}^\top$ is the spectral decomposition of $\mathbf{L}^\top \mathbf{L}$, it holds that

$$(\psi_i, \psi'_i)_{L^2_{\widehat{\mathbb{P}}_X \otimes \widehat{\mathbb{P}}_Y}} = \frac{1}{N} (\mathbf{L} \mathbf{v}_i)^\top (\mathbf{L} \mathbf{v}_{i'}) = \delta_{i,i'} \frac{\lambda_i}{N}. \quad (27)$$

Moreover, we readily infer

$$\langle \psi_i, \psi'_i \rangle_{\mathcal{H}} = \mathbf{v}_i^\top \mathbf{U}^\top \mathbf{K}(\mathbf{p}, \mathbf{p}) \mathbf{U} \mathbf{v}_{i'} = \delta_{i,i'}$$

due to $\mathbf{U}^\top \mathbf{K}(\mathbf{p}, \mathbf{p}) \mathbf{U} = \mathbf{I}$. This means, the constructed basis $\{\psi_i\} \subset V_\varepsilon$ is indeed orthogonal with respect to the \mathcal{H} -inner product and with respect to the $L^2_{\widehat{\mathbb{P}}_X \otimes \widehat{\mathbb{P}}_Y}$ -inner product at the same time. Hence, this basis is the discrete analogue of the spectral basis of the reproducing kernel. The cost for assembling the matrix $\mathbf{L}^\top \mathbf{L}$ is $\mathcal{O}(Nm^2)$, while the cost of the spectral decomposition is $\mathcal{O}(m^3)$. Hence, given that $m \leq N$, the overall cost for computing the double orthogonal basis $\{\psi_i\}_i^m$ is $\mathcal{O}(Nm^2)$.

In summary, the basis $\{\psi_i\}_{i=1}^m$ is easily computable and the approximation error in V_ε is rigorously controllable by the decay of the trace in the pivoted Cholesky decomposition, cp. Theorem 3.4. We remark that there also exist a-priori estimates on the rank m for a given accuracy ε if the eigenvalues of \mathbf{K} decay sufficiently fast, see Foster et al. (2009); Harbrecht et al. (2012). Another very important feature of the particular basis is that it considerably speeds up the optimization of (15), since the quadratic form $\mathbf{h}^\top \langle (J^* J + \lambda) \psi, \psi \rangle_{\mathcal{H}} \mathbf{h}$ in (15) is diagonal.

In light of the discussion at the end of Section 4, we next provide some bounds on the basis functions introduced above. Since the Newton basis is an orthonormal basis in \mathcal{H} , we know from the proof of Theorem 3.4 that

$$P_m^2(z) := k(z, z) - \sum_{i=1}^m N_i^2(z) \geq 0,$$

where P_m is the power function from Pazouki and Schaback (2011). In particular, we have $P_0^2(z) \geq P_1^2(z) \geq \dots \geq 0$ for all $z \in \mathcal{Z}$ and hence

$$N_i^2(z) = P_{i-1}^2(z) - P_i^2(z) \leq P_{i-1}^2(z) \leq k(z, z). \quad (28)$$

If $z_{p_i} = \arg \max_{z \in \mathcal{Z}} P_{i-1}(z)$, there even holds $N_i^2(z) \leq N_i^2(z_{p_i}) = P_{i-1}^2(z_{p_i})$ for all $z \in \mathcal{Z}$, cp. Pazouki and Schaback (2011). In this case, it is easy to see that

$$N_m^2(z_{p_m}) \leq N_{m-1}^2(z_{p_{m-1}}) \leq \dots \leq N_1^2(z_{p_1}) = k(z_{p_1}, z_{p_1}).$$

We emphasize, however, that the bound (28) is valid independently of the choice of the particular pivot points z_{p_1}, \dots, z_{p_m} . Moreover, the doubly orthogonal basis (26) satisfies

$$\begin{aligned} |\psi_i(z)| &= |\mathbf{N}(z) \mathbf{v}_i| \leq \sum_{j=1}^m |N_j(z)| \cdot |v_{i,j}| \\ &\leq \left(\sum_{j=1}^m N_j^2(z) \right)^{\frac{1}{2}} \cdot \left(\sum_{j=1}^m v_{i,j}^2 \right)^{\frac{1}{2}} = \left(\sum_{j=1}^m N_j^2(z) \right)^{\frac{1}{2}} = \sqrt{k(z, z) - P_m^2(z)}. \end{aligned}$$

Although the pivoted Cholesky decomposition already results in a major improvement of the computational cost, the required rank m might still be fairly large. For a tensor product kernel, however, the computational cost can be reduced further by applying the discussed algorithms to k_X and k_Y separately. If we denote the corresponding kernel matrices by $\mathbf{K}_X := [k_X(x_i, x_s)]_{i,s=1}^n$ and $\mathbf{K}_Y := [k_Y(y_j, y_t)]_{j,t=1}^n$, then

$$\mathbf{K} = \mathbf{K}_X \otimes \mathbf{K}_Y.$$

Importantly, we never need to fully assemble the matrices \mathbf{K}_X and \mathbf{K}_Y , but only as many columns as are necessary to reach the precision threshold ε in Algorithm 1. If the corresponding Cholesky factors are denoted by \mathbf{L}_X and \mathbf{L}_Y with ranks m_X and m_Y , then it furthermore holds

$$\mathbf{K} \approx \mathbf{L}\mathbf{L}^\top = (\mathbf{L}_X \otimes \mathbf{L}_Y)(\mathbf{L}_X \otimes \mathbf{L}_Y)^\top.$$

Instead of storing the rank $m = m_X m_Y$ matrix \mathbf{L} , it is sufficient to store the matrices \mathbf{L}_X and \mathbf{L}_Y , reducing the memory requirements from $\mathcal{O}(mn^2)$ to $\mathcal{O}((m_X + m_Y)n)$, while the computational cost is reduced from $\mathcal{O}((m_X m_Y)^2 n^2)$ to $\mathcal{O}(m_X^2 + m_Y^2)n$. Similarly, the biorthogonal basis \mathbf{B} , cp. Algorithm 2, can be written as $\mathbf{B} = \mathbf{B}_X \otimes \mathbf{B}_Y$, where \mathbf{B}_X and \mathbf{B}_Y are the biorthogonal bases of \mathbf{L}_X and \mathbf{L}_Y , respectively. Consequently, as the spectral decomposition of $\mathbf{L}^\top \mathbf{L}$ can also be factorized by means of the Kronecker product, we obtain for the doubly orthogonal basis ψ_m the identity

$$\psi_m = \psi_X \otimes \psi_Y,$$

where ψ_X and ψ_Y are the doubly orthogonal bases induced by \mathbf{L}_X and \mathbf{L}_Y , respectively. If we denote the corresponding subspaces by V_X and V_Y , we finally arrive at

$$V_\varepsilon = V_X \otimes V_Y.$$

In the next section, we detail our implementation, along with computational guidelines and recommendations.

6 Implementation

In this section, we discuss the implementation and several simplifications that result from our particular kernel choice and the choice of basis for the subspace V_ε . Thereafter, we establish efficiency and precision comparisons.

In all numerical experiments we adhere to the recommendations given in the previous section, and determine m_X and m_Y from applying Algorithm 2 separately to \mathbf{K}_X and \mathbf{K}_Y , respectively, for the same parameter ε .

Throughout we use the doubly orthogonal basis (26), $\psi_m = \phi \mathbf{B} \mathbf{V} =: \phi \mathbf{Q}$. In particular, we can represent any function $h_V \in V_\varepsilon$ as $\psi_m \mathbf{h}$, $\mathbf{h} \in \mathbb{R}^m$ from (18). We also

keep in mind the sample points z_{i_1}, \dots, z_{i_m} selected in Theorem 5.2. From (21)–(25) the sample version of the optimization problem (15) can be realized via

$$\begin{aligned}\langle \widehat{J}_0^* 1, h \rangle_{\mathcal{H}} &= \frac{1}{n} \sum_{i=1}^n [k(z_{i_1}, (x_i, y_i)), \dots, k(z_{i_m}, (x_i, y_i))] \mathbf{Q} \mathbf{h} \\ &= \int_{\mathcal{Z}} [k(z_{i_1}, z), \dots, k(z_{i_m}, z)] \mathbf{Q} \mathbf{h} \widehat{\mathbb{P}}_0(dz),\end{aligned}\quad (29)$$

$$\begin{aligned}\langle \widehat{J}^* p, h \rangle_{\mathcal{H}} &= \frac{1}{n^2} \sum_{i,j=1}^n p_{i,j} [k(z_{i_1}, (x_i, y_j)), \dots, k(z_{i_m}, (x_i, y_j))] \mathbf{Q} \mathbf{h} \\ &= \int_{\mathcal{Z}} [k(z_{i_1}, z), \dots, k(z_{i_m}, z)] \mathbf{P} \mathbf{Q} \mathbf{h} (\widehat{\mathbb{P}_X \otimes \mathbb{P}_Y})(dz),\end{aligned}\quad (30)$$

where $\mathbf{P} := [p_{i,j}]_{i,j=1}^n$, while the entry in (s, t) position of the matrix \mathbf{W} in $\langle \widehat{J}^* \widehat{J} h, h \rangle_{\mathcal{H}} = \mathbf{h}^\top \mathbf{Q}^\top \mathbf{W} \mathbf{Q} \mathbf{h}$ is given by

$$w_{s,t} = \frac{1}{n^2} \sum_{i,j=1}^n k(z_{i_s}, (x_i, y_j)) k(z_{i_t}, (x_i, y_j)) \quad (31)$$

$$= \int_{\mathcal{Z}} k(z_{i_s}, z) k(z_{i_t}, z) (\widehat{\mathbb{P}_X \otimes \mathbb{P}_Y})(dz) \quad (32)$$

and lastly

$$\langle h, h \rangle_{\mathcal{H}} = \mathbf{h}^\top \mathbf{Q}^\top \mathbf{K} \mathbf{Q} \mathbf{h}. \quad (33)$$

With the doubly orthogonal basis $\psi_m(z) := \phi(z) \mathbf{Q}$ defined in (26), we can now concisely write the objective function of optimization problem (15) as

$$\begin{aligned}& 2 \left(\int_{\mathcal{Z}} \phi(z) \widehat{\mathbb{P}_X \otimes \mathbb{P}_Y}(dz) - \int_{\mathcal{Z}} \phi(z) \widehat{\mathbb{P}}_0(dz) \right) \mathbf{Q} \mathbf{h} \\ & + \mathbf{h}^\top \mathbf{Q}^\top \left(\int_{\mathcal{Z}} \phi(z)^\top \phi(z) \widehat{\mathbb{P}_X \otimes \mathbb{P}_Y}(dz) + \lambda \mathbf{K} \right) \mathbf{Q} \mathbf{h} \\ & = 2 \left(\int_{\mathcal{Z}} \psi_m(z) \widehat{\mathbb{P}_X \otimes \mathbb{P}_Y}(dz) - \int_{\mathcal{Z}} \psi_m(z) \widehat{\mathbb{P}}_0(dz) \right) \mathbf{h} + \mathbf{h}^\top (\mathbf{\Lambda} + \lambda \mathbf{I}) \mathbf{h}.\end{aligned}\quad (34)$$

As a benefit of the doubly orthogonal basis, the quadratic form is

$$\mathbf{h}^\top (\mathbf{\Lambda} + \lambda \mathbf{I}) \mathbf{h},$$

where the diagonal matrix $\mathbf{\Lambda}$ is given by (27). This greatly improves stability and speed of the optimization program, since there are only m , rather than $m(m+1)/2$ entries to compute with no cross terms. This enables us to obtain rapid solutions using standard quadratic solvers.

Owing to the tensor product structure of the reproducing kernel, we can formulate normalization constraints (5) and (6) on V_X and V_Y in accordance with Section 4 as follows: From (19) in Lemma 4.1, with $\mathbf{h} = \text{vec } \mathbf{H}$, we can write conditions (5) as

$$(\text{diag } \mathbf{1} \otimes I_Y \psi_X) \mathbf{h} =: \mathbf{\Gamma}_X \mathbf{h} = \mathbf{0} \Leftrightarrow (I_X \psi_Y) \mathbf{H} = \mathbf{0} \quad (35)$$

and similarly (6) as

$$(I_X \psi_Y \otimes \text{diag } \mathbf{1}) \mathbf{h} =: \mathbf{\Gamma}_Y \mathbf{h} = \mathbf{0} \Leftrightarrow \mathbf{H} (I_Y \psi_X)^\top = \mathbf{0}. \quad (36)$$

Together with condition (20), we thus obtain the normalization and positivity certificates demanded by (5), (6) and (7). To further lighten notation, denote by

$$\boldsymbol{\alpha} := \int_{\mathcal{Z}} \psi_m(z) \widehat{\mathbb{P}_X \otimes \mathbb{P}_Y}(\text{d}z) - \int_{\mathcal{Z}} \psi_m(z) \widehat{\mathbb{P}_0}(\text{d}z), \quad \mathbf{A} := \frac{1}{2}(\boldsymbol{\Lambda} + \lambda \mathbf{I}).$$

With a constant prior $p = 1$, the primal optimization problem then reads

$$\begin{aligned} & \underset{\mathbf{h}, \mathbf{h}^+, \mathbf{h}^- \in \mathbb{R}^m}{\text{minimize}} \quad \boldsymbol{\alpha} \mathbf{h} + \frac{1}{2} \mathbf{h}^\top \mathbf{A} \mathbf{h}. \\ & \text{subject to} \quad \mathbf{\Gamma}_X \mathbf{h} = \mathbf{0}, \mathbf{\Gamma}_Y \mathbf{h} = \mathbf{0}, \\ & \quad \mathbf{h} = \mathbf{h}^+ - \mathbf{h}^-, \\ & \quad \mathbf{a}^\top \mathbf{h}^+ - \mathbf{b}^\top \mathbf{h}^- + 1 \geq 0, \\ & \quad \mathbf{h}_i^+ \geq 0, \mathbf{h}_i^- \geq 0, \end{aligned} \quad (37)$$

where \mathbf{a}, \mathbf{b} are bounds depending on the particular kernels \mathbf{K}_X and \mathbf{K}_Y chosen. This is a standard linearly constrained quadratic optimization problem with a *diagonal* quadratic form. Note that without the constraints, the minimization can be performed in closed form as

$$\mathbf{h} = -\mathbf{A}^{-1} \boldsymbol{\alpha}^\top. \quad (38)$$

7 Numerical experiments

In this section, we put our low-rank conditional distribution embedding to several numerical tests. To illustrate the general applicability of our framework to various types of problems, we perform *prediction* and in a separate exercise *classification*. As the basis for both investigations serve draws from a three-dimensional random variable $Z \sim \mathcal{N}(\boldsymbol{\mu}, \boldsymbol{\Sigma})$, where we set for simplicity $\boldsymbol{\mu} = [0, 0, 0]^\top$, $\text{diag } \boldsymbol{\Sigma} = [1/25, 1/25, 1/25]$ and consider different dependence scenarios through the pairwise correlations ρ_{XY}, ρ_{XZ} , and ρ_{YZ} .

Conditional expectations

In the first type of investigation, we consider the conditional distribution of $Y_1, Y_2|X$, where $Y_1 = Z_1, Y_2 = Z_2$, and $X = Z_3$ are jointly normal. We perform tests with respect to scalability, speed, and quality of conditional moments estimated. We perform all tests regarding speed with Gaussian kernels k_X and k_Y , the parameters σ_X and σ_Y of which we sample from a uniform distribution $\mathcal{U}(10^{-5}, 0.1)$. In all other tests, we determine the kernel parameters from a validation procedure. Except for the coefficients of the traditional embedding described in (42), we set the regularization parameter $\lambda = 0$ and consider instead different tolerances ε in Algorithm 1 sampled from a uniform distribution $\mathcal{U}(10^{-5}, 0.1)$. In fact, these tolerances serve as a natural regularization for our formulation, as they control how many, and which, data points are considered for the low-rank conditional distribution embedding.

To obtain test functions of which to estimate conditional expectations, we consider the event

$$A := aY_1 \leq bY_2 + c. \quad (39)$$

The conditional expectation of the indicator of the event

$$\mathbb{E}[\mathbb{1}_A|X] = \mathbb{P}(Y_1 \leq Y_2 + a|X),$$

allows to measure the efficacy of the competing embedding approaches with respect to important dimensions. First, with the true conditional probability known, it measures the predictive power. Second, it is easy to check positivity. Third, by setting $a = b = c = 0$ such that the event is always true, we can investigate how close the distribution embeddings are to being normalized. We discuss these aspects in detail below.

For any test we simulate realizations from the joint distribution of $Z := (Y_1, Y_2, X)$ with the number of data points varying between 100 and 10^6 . For each run, we distinguish between three different samples: training, validation, and testing. We denote the realizations making up these samples by

$$\begin{aligned} z^{\text{train}} &:= (z_1^{\text{train}}, \dots, z_{n_{\text{train}}}^{\text{train}}), \\ z^{\text{val}} &:= (z_1^{\text{val}}, \dots, z_{n_{\text{val}}}^{\text{val}}), \\ z^{\text{test}} &:= (z_1^{\text{test}}, \dots, z_{n_{\text{test}}}^{\text{test}}), \end{aligned}$$

respectively. Stacking

$$\mathbf{t}(Y_1, Y_2) := \begin{bmatrix} \mathbb{1}_{Y_1 \leq Y_2 - 0.5} \\ \mathbb{1}_{Y_1 \leq Y_2 - 0.6} \\ \mathbb{1}_{Y_1 \leq Y_2 - 0.7} \\ \mathbb{1}_{0 \leq 0} \end{bmatrix}, \quad (40)$$

and with coefficients \mathbf{h} computed from z^{train} , the objective function for validation is taken to be

$$\sum_{i=1}^{n_{\text{val}}} \|\mathbf{t}(y_{1i}^{\text{val}}, y_{2i}^{\text{val}}) - \mathbb{E}^{\mathcal{M}}[\mathbf{t}(Y_1, Y_2)|X = x_i^{\text{val}}]\|_2^2, \quad (41)$$

where \mathcal{M} is a placeholder for the expectation induced by four different models: 1) the constrained conditional distribution embedding from (37), 2) its unconstrained counterpart (without conditions (6), (5), and (7) imposed), 3) its normalized counterpart (without condition (7) imposed), and 4) the traditional conditional distribution embedding from Song et al. (2009). From the realizations of X , we also compute the conditional expectations $\mathbb{E}[\mathbf{t}(Y_1, Y_2)|X]$ obeying the true population moments $\boldsymbol{\mu}$ and $\boldsymbol{\Sigma}$. In the following section, we first discuss run times of the training step, i.e., the determination of \mathbf{h} using z^{train} .

Speed and scalability

Optimization problem (37) requires the use of a conic solver for given kernel parameters and data to obtain \mathbf{h} . As a first test, we investigate whether this imposes computational barriers. For a relative comparison, we employ the traditional conditional expectation operator $\mu_{Y|X} \in \mathcal{H}_Y$ from Song et al. (2009), whose coefficients for observed data points $z_1^{\text{train}}, \dots, z_{n_{\text{train}}}^{\text{train}}$ are given by the matrix

$$\mathbf{M} := (\mathbf{K}_X + \lambda \mathbf{I})^{-1}. \quad (42)$$

For any $f \in \mathcal{H}_Y$ the conditional expectation $f(Y)|X = x$ is then evaluated as

$$\mathbb{E}[f(Y)|X = x] = \langle f, \mu_{Y|X=x} \rangle_{\mathcal{H}_Y} = [f(y_1^{\text{train}}), \dots, f(y_{n_{\text{train}}}^{\text{train}})] \mathbf{M} \begin{bmatrix} k_X(x_1^{\text{train}}, x) \\ \vdots \\ k_X(x_{n_{\text{train}}}^{\text{train}}, x) \end{bmatrix}.$$

This construction is elegant and efficient, but also has its downsides. For instance, the constant function $f \equiv 1$ is not a member of the Gaussian \mathcal{H}_Y that we use, see Minh (2010), and therefore would preclude evaluation of test functions (39). In our construction, any constant is encoded through the prior p , while the RKHS part is orthogonal to constants.

A sparse version of the traditional distribution embedding is introduced in Grünewälder et al. (2012). However, their approach necessitates the full kernel matrices \mathbf{K}_X and \mathbf{K}_Y in an iterated algorithm. The times below for the computation of a single coefficient matrix \mathbf{M} in (42) are therefore to be understood as a lower bound for the sparse version. Our implementation is executed on an 18-core Intel i9-10980XE processor with 64 GB of memory using a fully threaded Intel Math Kernel Library (MKL) along with the GCC compiler. We use Gurobi Optimization (2021) to numerically solve (15). Run time statistics are computed from 100 runs.

Figure 1 shows the computation times of the kernel embeddings as a function of the number of data points n_{train} on a log scale. We denote by *constrained* the solution obtained from (37), by *unconstrained* the solution obtained without imposing normalization and positivity, and by *traditional* the computation of \mathbf{M} in (42). While the unconstrained solution can be obtained from inverting a matrix (along with the

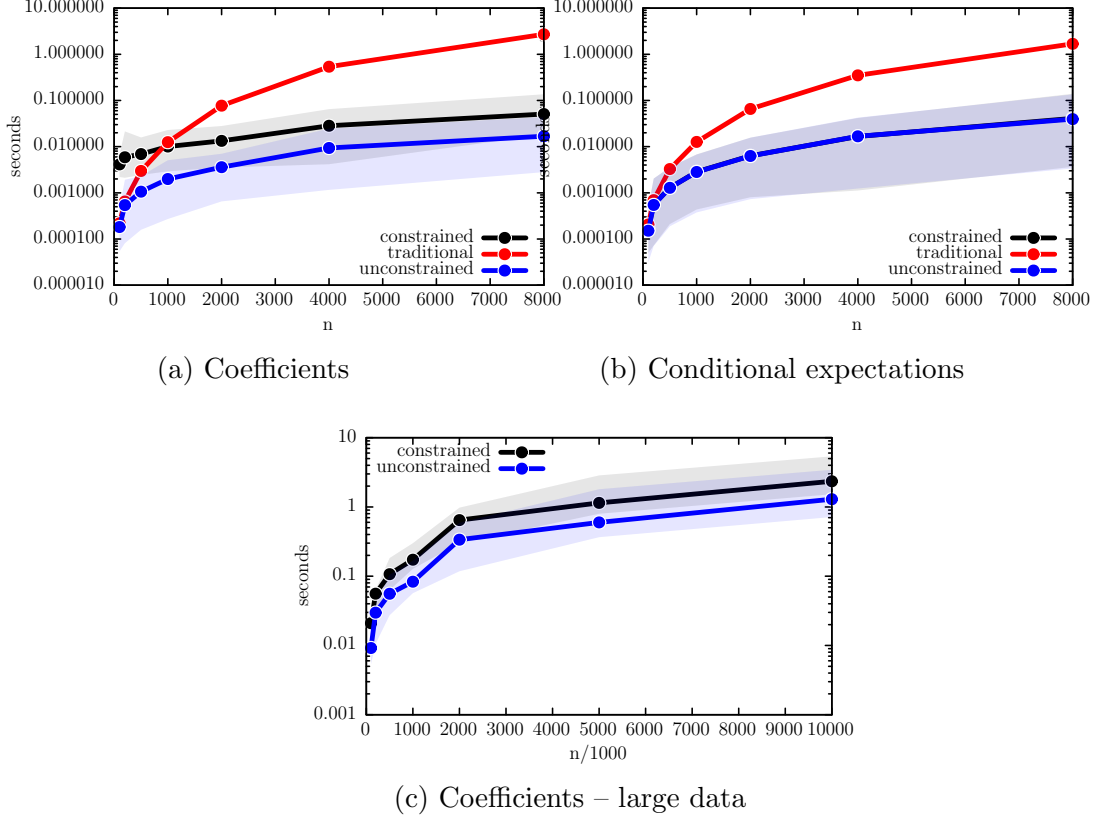


Figure 1: Computation times. Panel **a** shows computation times in seconds to solve for the coefficients \mathbf{h} from (37) (constrained), (38) (unconstrained), respectively the coefficient matrix \mathbf{M} from (42). Panel **b** shows computation times to evaluate the conditional expectations of a vector of four test functions given in (39). Panel **c** shows run times times for the same calculations, but larger test sample sizes. As these large data sets are computationally intractable for the traditional conditional distribution embedding, times are shown only for the constrained and unconstrained specifications. Confidence bands are computed from 100 optimizations on data sets generated from $\mathcal{N}(\boldsymbol{\mu}, \boldsymbol{\Sigma})$ and randomly generated kernel, regularization, and threshold parameters. For all three panels lower is better. The shaded areas show 5% to 95% confidence bands.

solution that is only normalized, that is not reported here), but contrary to the traditional embedding this matrix is diagonal due to the doubly orthogonal basis.

It shows that for $n_{\text{train}} \leq 1000$ the implementations are comparably fast. With larger sample sizes, the adaptive low-rank embedding shows clear computational advantages. For large n_{train} , the traditional kernel embedding facilitates very large densely populated matrices that pose challenges to computer memory. As our low-rank distribution embedding does not make use of the full kernel matrix, but only of certain selected columns, large values of n_{train} are less problematic. Consequently, Figure 1c shows computation times only for the constrained and unconstrained embeddings proposed in this paper for up to 10 million data points. This number of data points would clearly be computationally intractable with the traditional embedding that makes use of the full kernel matrices. With the constrained and unconstrained embedding, also larger sample sizes are feasible (and fast to compute), that would preclude application of the traditional embedding (42).

Accuracy and structural preservation

In this section, we consider the empirical accuracy of the probability embeddings, relate it to computational, as well as structural considerations. To this end, we validate kernel, regularization, and threshold parameters via the objective (41) and subsequently compare the model-implied conditional expectation to the true conditional expectations evaluated at the population moments. For the distribution embeddings introduced in this paper, this entails validating 2 parameters for the Gaussian kernels \mathcal{H}_X and \mathcal{H}_Y , as well as the threshold parameter ε , hence three in total, since we set $\lambda = 0$. For the traditional distribution embedding, the parameter of \mathcal{H}_Y is irrelevant, necessitating validation only of the \mathcal{H}_X parameter, as well as the regularization parameter λ .

We assess the accuracy of the predictions from the oracle criterion

$$\frac{1}{n_{\text{test}}} \sum_{i=1}^{n_{\text{test}}} \left\| \mathbb{E}^{\mathcal{M}} [\mathbf{t}(Y_1, Y_2) | X = x_i^{\text{test}}] - \mathbb{E} [\mathbf{t}(Y_1, Y_2) | X = x_i^{\text{test}}] \right\|_2^2. \quad (43)$$

Figure 2 shows empirical results for the different types of embeddings across different values of n_{train} for three different dependence scenarios, 1) *low*, $\rho_{XY} = \rho_{XZ} = \rho_{YZ} = 0$, 2) *med.*, $\rho_{XY} = 0.3, \rho_{XZ} = -0.3, \rho_{YZ} = 0.3$, and 3) *high*, $\rho_{XY} = 0.7, \rho_{XZ} = 0.7, \rho_{YZ} = -0.7$. A-priori the constrained embedding developed in this paper is to be expected to perform worse for data with higher correlations, as the RKHS part h needs to deform the Radon-Nikodym derivative (12) more in this case, subject to the positivity constraint.

The left column confirms this prior, but shows that the constrained embedding works very well also for highly dependent data, as its error norm is consistently below the traditional embedding, and the two unconstrained/partially constrained versions, except in the mid-correlation case, where it behaves worse for $n_{\text{train}} = 1000$. Notably,

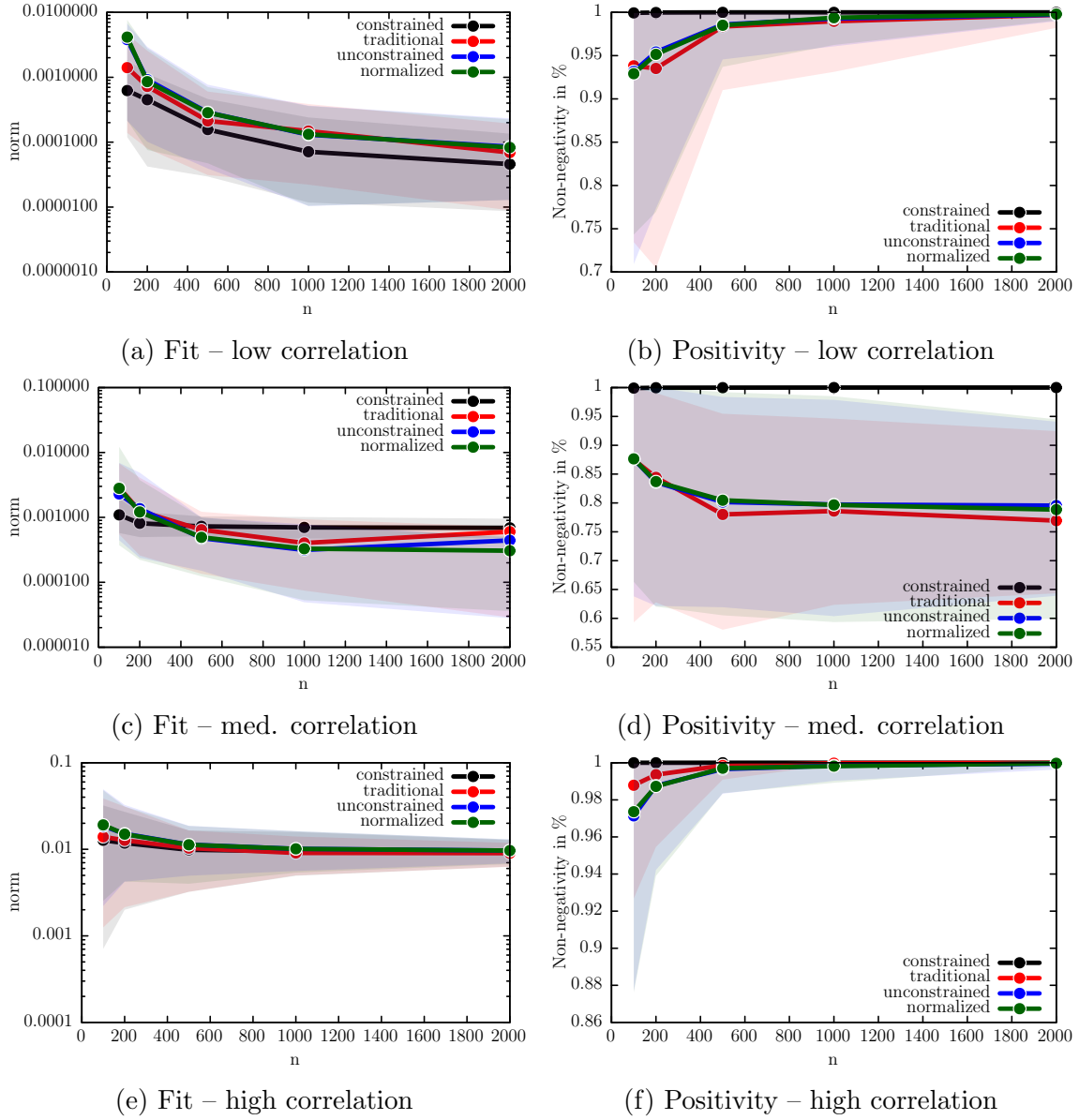


Figure 2: Empirical accuracy. The figure shows empirical accuracy according to criterion (43) as a function of n_{train} . Confidence bands are computed from 100 optimizations on randomly generated sample paths from $\mathcal{N}(\boldsymbol{\mu}, \boldsymbol{\Sigma})$ for three correlation parameterizations: 1) *low*, $\rho_{XY} = \rho_{XZ} = \rho_{YZ} = 0$, 2) *med.*, $\rho_{XY} = 0.3, \rho_{XZ} = -0.3, \rho_{YZ} = 0.3$, and 3) *high*, $\rho_{XY} = 0.7, \rho_{XZ} = 0.7, \rho_{YZ} = -0.7$. The three models compared are the distribution embedding (37) (constrained), without constraints (38) (unconstrained), with normalization but no positivity imposed (normalized), and the conditional distribution embedding from Song et al. (2009) (traditional). The panels in the left column show the oracle norm (43), while the right columns show the percentage with which all probabilities are non-negative. The shaded areas show 5% to 95% confidence bands.

the constrained embedding works considerably better for a small number of data points in the range of 100 or 200 samples, where the probabilistic constraints help.

Many applications require estimates of conditional moments to obey the same structure that any moment sequence generated by a probability distribution would satisfy. For instance, any population covariance matrix is positive semidefinite (provided there are more data points than the dimension of state variables). Consequently, any estimate of a covariance matrix used in an application relying on this property, for example in portfolio optimization, should conceivably be positive semidefinite as well. Checking positivity of the conditional expectations of the test functions (39) gives a direct indication of this property.

There is no mechanism in the determination of the coefficient matrix \mathbf{M} in (42) that ensures that moments estimated with traditional distribution embedding obey the same structure as moments coming from a probability distribution. Another issue is the estimation of conditional expectations of constants. Any estimator should reasonably be expected to ensure that (conditional) expectations of constants yield the same constants.

The right column in Figure 2 gives the percentage with which all model-implied probabilities are non-negative. It shows that in particular for a small number of data points, the unconstrained embeddings substantially violate positivity. For the mid-correlation scenario, these violations persist also on average across the number of data points. Figure 3 shows for the same mid-correlation scenario the average deviation of $\mathbb{E}^{\mathcal{M}}[1|X]$ from one and suggests a bias that does not vanish with the number of data points.

Finally, Figure 4 shows that the quality of the probability representation is not immediately related to m , the dimension of V_ε which is due to the exponential decay of the spectrum of the Gaussian kernel.

Classification

Classification is a task with long history in statistics and learning, and of prominent importance in machine learning. Starting from our random variables Z introduced at the beginning of this section, we set $X_1 = Z_1, X_2 = Z_2$, and $Y = Z_3$ for this exercise and consider $\text{sgn } Y|X_1, X_2$. For both, the traditional distribution embedding, as well as the one proposed in this paper, the probability is estimated nonparametrically with $y \in \{-1, 1\}$ as

$$\mathbb{P}^{\mathcal{M}}(\text{sgn } Y = y|X_1, X_2) = \mathbb{E}^{\mathcal{M}}[\mathbb{1}(\text{sgn } Y = y)|X_1, X_2]. \quad (44)$$

In addition to the traditional distribution embedding, we consider here also kernel logistic regression (Zhu and Hastie, 2005), where for $f \in \mathcal{H}_X$ the conditional probability is parameterized as

$$\mathbb{P}^{\text{klr}}(\text{sgn } Y = y|f(X_1, X_2)) = \frac{1}{1 + \exp(-yf(X_1, X_2))},$$

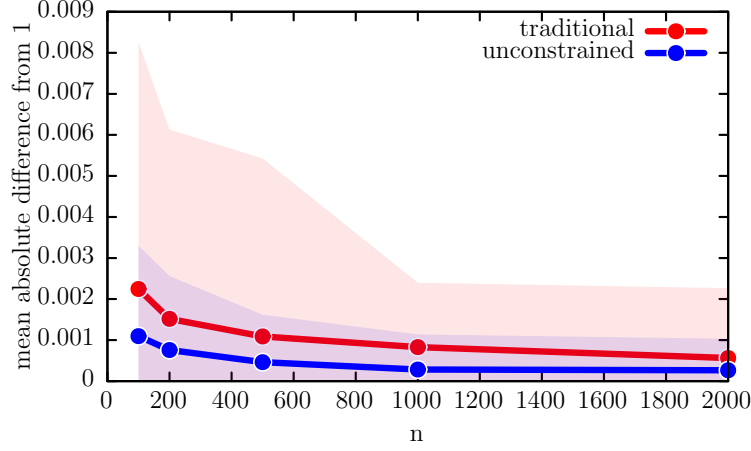


Figure 3: Structural properties. The figure compares the unconstrained distribution embedding from this paper to the traditional embedding from [Song et al. \(2009\)](#) with respect to their structural implications. It shows the mean absolute deviation $|\mathbb{E}^{\mathcal{M}}[1|X] - 1|$ computed from the same 100 runs as Figure 2. The constrained distribution embedding, as well as the normalized one, satisfy $|\mathbb{E}^{\mathcal{M}}[1|X] - 1| = 0$ \mathbb{P}_X a.s., and are therefore not depicted. The shaded areas show 5% to 95% confidence bands.

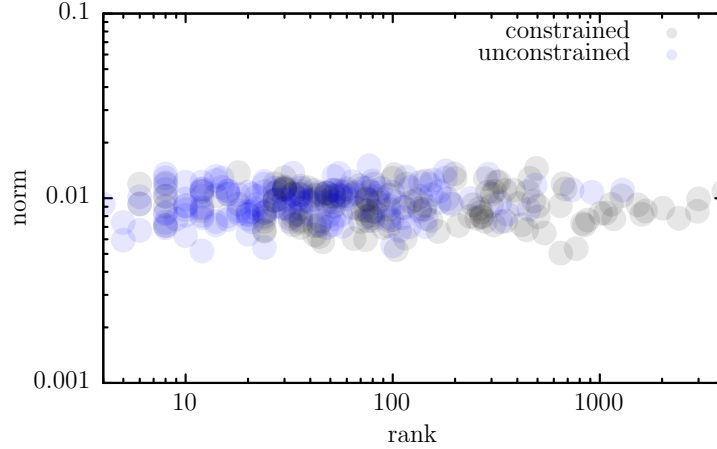


Figure 4: Rank of distribution embedding. The figure shows a scatterplot of the dimension m of \mathbf{h} against the criterion (43) for both the constrained and the unconstrained distribution embedding, (37) and (38). Both the x-axis and the y-axis are depicted on log scales. The data points are computed from the same 100 runs that make up Figure 2.

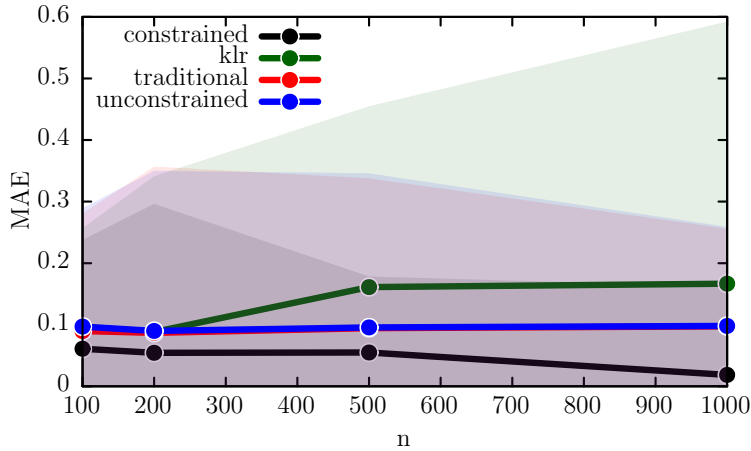


Figure 5: Classification. The figure shows the mean absolute deviation of a perfect classification as a function of n_{train} . Confidence bands are computed from optimizations on 100 data sets generated from $\mathcal{N}(\boldsymbol{\mu}, \boldsymbol{\Sigma})$. The statistics are computed for $n_{\text{val}} = n_{\text{train}}$, and $n_{\text{test}} = 1000$. The four models compared are the distribution embedding (37) (constrained), without constraints (38) (unconstrained), and the conditional distribution embedding from Song et al. (2009) (traditional), and kernel logistic regression (klr). Lower is better. The shaded areas show 5% to 95% confidence bands.

for $y \in \{-1, 1\}$. For this classification exercise, we validate four contending models 1) the constrained, and 2) unconstrained distribution embedding introduced in this paper, 3) the traditional distribution embedding, and the 4) kernel logistic regression, with the logistic loss $-\log \mathbb{P}^{\mathcal{M}}$, where the placeholder \mathcal{M} is assumed here to accommodate also the kernel logistic regression. For the logistic kernel regression, the logistic loss is also used as the criterion to obtain the kernel parameters via

$$\mathbf{h}^{\text{klr}} = \arg \min_{\mathbf{h} \in \mathbb{R}^{n_{\text{test}}}} \frac{1}{n_{\text{test}}} \sum_{i=1}^{n_{\text{test}}} \log(1 + \exp(-y_i(\mathbf{K}_X \mathbf{h})_i)) + \lambda \mathbf{h}^\top \mathbf{K}_X \mathbf{h},$$

where we use the MOSEK ApS (2021) optimizer to minimize over the exponential and quadratic cones.

Figure 5 shows the results up to $n_{\text{train}} = 1000$. Logistic kernel regression becomes computationally difficult for a greater number of data points. The mean absolute deviation from perfect classification is relatively small for all contending models. This is due to the mean $\boldsymbol{\mu}$ of the underlying random variables Z being non-zero in general. The unconstrained and traditional distribution embeddings are almost indistinguishable with respect to their mean absolute deviation and the confidence band. The constrained distribution embedding performs best here, likely due to its structural benefits due to normalization and positivity. Logistic kernel mean regression shows the worst performance on average, and the widest confidence bands. At least for the

present problem at hand, the parametric specification leaves a disadvantage.

8 Conclusions

We have proposed a new approach to estimate joint and conditional distributions in RKHS employing adaptive low-rank techniques. By considering tensor product RKHS, our framework is well equipped to handle large samples, while satisfying positivity and normalization as important structural traits induced by probability distributions. We have shown that the presented approach is computationally efficient, versatile and precise.

References

- ALMEIDA, C. AND P. SCHNEIDER (2021): “Constrained polynomial likelihood,” Work in progress, Princeton University, USI Lugano and SFI.
- BACH, F. AND M. JORDAN (2002): “Kernel independent component analysis,” *Journal of Machine Learning Research*, 3, 1–48.
- BEEBE, N. AND J. LINDERBERG (1977): “Simplifications in the generation and transformation of two-electron integrals in molecular calculations,” *International Journal of Quantum Chemistry*, 12, 683–705.
- BERLINET, A. AND C. THOMAS-AGNAN (2004): *Reproducing Kernel Hilbert Spaces in Probability and Statistics*, Boston, MA: Springer US, 1–54.
- BOUDABSA, L. AND D. FILIPOVIĆ (2019): “Machine learning with kernels for portfolio valuation and risk management,” *Swiss Finance Institute Research Paper*.
- FOSTER, L., A. WAAGEN, N. ALJAZ, M. HURLEY, A. LUIS, J. RINSKY, C. SATYAVOLU, AND M. COM (2009): “Stable and Efficient Gaussian Process Calculations,” *Journal of Machine Learning Research*, 10, 857–882.
- GRÜNEWÄLDER, S., G. LEVER, L. BALDASSARRE, S. PATTERSON, A. GRETTON, AND M. PONTIL (2012): “Conditional mean embeddings as regressors,” in *Proceedings of the 29th International Conference on Machine Learning*, New York: Omnipress, 1823–1830.
- GUROBI OPTIMIZATION, L. (2021): “Gurobi Optimizer Reference Manual,” .
- HARBRECHT, H., M. PETERS, AND R. SCHNEIDER (2012): “On the low-rank approximation by the pivoted Cholesky decomposition,” *Applied Numerical Mathematics*, 62, 28–440.
- KLEBANOV, I., I. SCHUSTER, AND T. J. SULLIVAN (2020): “A Rigorous Theory of Conditional Mean Embeddings,” *SIAM Journal on Mathematics of Data Science*, 2, 583–606.

- KOPPEL, A., K. ZHANG, H. ZHU, AND T. BAŞAR (2019): “Projected Stochastic Primal-Dual Method for Constrained Online Learning With Kernels,” *IEEE Transactions on Signal Processing*, 67, 2528–2542.
- MARTEAU-FEREY, U., F. BACH, AND A. RUDI (2020): “Non-parametric Models for Non-negative Functions,” .
- MICCHELLI, C. A. AND M. A. PONTIL (2005): “On Learning Vector-Valued Functions,” *Neural Computation*, 17, 177–204.
- MINH, H. Q. (2010): “Some Properties of Gaussian Reproducing Kernel Hilbert Spaces and Their Implications for Function Approximation and Learning Theory,” *Constructive Approximation*, 32, 1432–0940.
- MOSEK APS (2021): *MOSEK Fusion API for C++ 9.2.37*.
- MÜLLER, S. AND R. SCHABACK (2009): “A Newton basis for Kernel spaces,” *Journal of Approximation Theory*, 161, 645–655.
- MUZELLEC, B., F. BACH, AND A. RUDI (2021): “A Note on Optimizing Distributions using Kernel Mean Embeddings,” .
- PARK, J. AND K. MUANDET (2020): “A measure-theoretic approach to kernel conditional mean embeddings,” Working paper, Max Planck Institute for Intelligent Systems.
- PAULSEN, V. I. AND M. RAGHUPATHI (2016): *An introduction to the theory of reproducing kernel Hilbert spaces*, vol. 152 of *Cambridge Studies in Advanced Mathematics*, Cambridge University Press, Cambridge.
- PAZOUKI, M. AND R. SCHABACK (2011): “Bases for kernel-based spaces,” *Journal of Computational and Applied Mathematics*, 236, 575–588.
- SCHATTEN, R. (1960): *Norm ideals of completely continuous operators*, Berlin-Göttingen-Heidelberg: Springer.
- SCHUSTER, I., M. MOLLENHAUER, S. KLUS, AND K. MUANDET (2020a): “Kernel Conditional Density Operators,” in *Proceedings of the 23rd International Conference on Artificial Intelligence and Statistics (AISTATS) 2020*, ed. by S. Chiappa and R. Calandra, Online: PMLR, vol. 108 of *Proceedings of Machine Learning Research*, 993–1004.
- (2020b): “Kernel Conditional Density Operators,” in *Proceedings of the Twenty Third International Conference on Artificial Intelligence and Statistics*, ed. by S. Chiappa and R. Calandra, Online: PMLR, vol. 108 of *Proceedings of Machine Learning Research*, 993–1004.
- SONG, L., J. HUANG, A. SMOLA, AND K. FUKUMIZU (2009): “Hilbert Space Embeddings of Conditional Distributions with Applications to Dynamical Systems,” in *Proceedings of the 26th Annual International Conference on Machine Learning*, New York, NY, USA: Association for Computing Machinery, ICML 2009, 961–968.

ZHU, J. AND T. HASTIE (2005): “Kernel Logistic Regression and the Import Vector Machine,” *Journal of Computational and Graphical Statistics*, 14, 185–205.